bioRxiv preprint doi: https://doi.org/10.1101/505529; this version posted December 24, 2018. The copyright holder for this preprint (which was not certified by peer review) is the author/funder. All rights reserved. No reuse allowed without permission.

1 **Honey bee parasitic mite contains the sensory organ expressing ionotropic**
2 **receptors with conserved functions**
3
4 Jing Lei, Qiushi Liu, and Tatsuhiko Kadowaki*
5
6 Department of Biological Sciences, Xi'an Jiaotong-Liverpool University, 111 Ren'ai
7 Road, Suzhou Dushu Lake Higher Education Town, Jiangsu Province 215123, China
8
9 *Corresponding author:
10 Tatsuhiko Kadowaki
11 Department of Biological Sciences, Xi'an Jiaotong-Liverpool University
12 111 Ren'ai Road, Suzhou Dushu Lake Higher Education Town
13 Jiangsu Province 215123, China
14 TEL: 86 512 88161659, FAX: 86 512 88161899
15 E-mail: Tatsuhiko.Kadowaki@xjtlu.edu.cn
16

bioRxiv preprint doi: https://doi.org/10.1101/505529; this version posted December 24, 2018. The copyright holder for this preprint (which was not certified by peer review) is the author/funder. All rights reserved. No reuse allowed without permission.

17 **Abstract**

18 Honey bee parasitic mites (*Tropilaelaps mercedesae* and *Varroa destructor*) detect
19 temperature, humidity, and odor but the underlying sensory mechanisms are poorly
20 understood. To uncover how *T. mercedesae* responds to environmental stimuli inside a
21 hive, we identified the sensilla-rich sensory organ on the foreleg tarsus. The organ
22 contained four types of sensilla, which may respond to different stimuli based on their
23 morphology. We found the forelegs were enriched with mRNAs encoding sensory
24 proteins such as ionotropic receptors (IRs) and gustatory receptors (GRs), as well as
25 proteins involved in ciliary transport. We also found that *T. mercedesae* and *Drosophila*
26 *melanogaster* IR25a and IR93a are functionally equivalent. These results demonstrate
27 that the structures and physiological functions of ancient IRs have been conserved
28 during arthropod evolution. Our study provides insight into the sensory mechanisms of
29 honey bee parasitic mites, as well as potential targets for methods to control the most
30 serious honey bee pest.

31

bioRxiv preprint doi: https://doi.org/10.1101/505529; this version posted December 24, 2018. The copyright holder for this preprint (which was not certified by peer review) is the author/funder. All rights reserved. No reuse allowed without permission.

32 **Introduction**

33 The number of managed honey bee colonies has declined across North America and
34 Europe in recent years [1]. Pollination by honey bees is critical for maintaining
35 ecosystems and producing many agricultural crops [2,3]. Prevention of honey bee losses
36 has, therefore, become a major issue in apiculture and agriculture. Although there are
37 many potential causes for the observed declines, ectoparasitic mites are considered to be
38 major threats to the health of honey bees and their colonies [1,4]. *Varroa destructor* is
39 present globally (except Australia) and causes both abnormal brood development and
40 brood death in honey bee colonies [5]. The mites feed on hemolymph and also spread
41 honey bee viruses, particularly deformed wing virus (DWV) [6,7]. In many Asian
42 countries, another honey bee ectoparasitic mite, *Tropilaelaps mercedesae*, is also
43 prevalent in *Apis mellifera* colonies [8,9]. These two emerging parasites of *A. mellifera*
44 share many characteristics [10]. For example, they have similar reproductive strategies [11]
45 and both are vectors for DWV [12-15]. As a result, *T. mercedesae* or *V. destructor*
46 infestations have similar negative impacts on *A. mellifera* colonies [16-18]. Although *T.*
47 *mercedesae* is currently restricted to Asia, it has the potential to spread and establish
48 worldwide due to the global trade in honey bees.

49 *V. destructor* prefers temperatures of 32 ± 2.9 °C, reproduces best at
50 32.5-33.4 °C, and has been shown to discriminate temperature differences of 1 °C [19-21].
51 Furthermore, its reproduction also depends on humidity of 55-70 % [22]. These results
52 demonstrate thermo- and hygrosensation of *V. destructor* play important roles to adapt
53 to the honey bee hive environment; nevertheless, chemoreception must be most
54 important in the various interactions between mites and their honey bee hosts. For
55 example, *V. destructor* prefers to parasitize nurse bees rather than foragers during its
56 phoretic phase [23,24]. For its reproductive stage, it locates fifth instar honey bee larva and
57 enters the brood cell prior to capping [25]. These behaviors are considered to be mediated
58 by chemical cues derived from the adult bee, larva, and larval food. Since *T.*
59 *mercedesae* has a very similar life cycle to *V. destructor*, both honey bee mites should
60 be equipped with thermo-, hygro-, and chemosensation, as observed in other mite/tick
61 (Acari) species. Accordingly, *V. destructor* was found to have a sensilla-rich sensory
62 organ on the foreleg tarsus [26,27], which corresponds to Haller's organ in ticks [28].
63 Proteomic and transcriptomic characterization were conducted for the forelegs of *V.*
64 *destructor,* which identified potential semiochemical carriers and sensory proteins [29].

65 Ionotropic receptors (IRs) represent a subfamily of ionotropic glutamate
66 receptors (iGluRs), which are conserved ligand-gated ion channels. IRs have
67 specifically evolved in protostomes [30] and are best characterized in the fruit fly,

bioRxiv preprint doi: https://doi.org/10.1101/505529; this version posted December 24, 2018. The copyright holder for this preprint (which was not certified by peer review) is the author/funder. All rights reserved. No reuse allowed without permission.

68 *Drosophila melanogaster*. Most IRs are expressed in sensory neurons and function as
69 chemoreceptors to detect various odorants and tastants [31,32]. Recent studies have also
70 demonstrated that IR21a, IR40a, IR68a, IR93a, and IR25a are critical for thermo- and
71 hygrosensation, suggesting that IRs have diverse physiological roles as well as gating
72 mechanisms [33-36]. IR25a has the same protein domains as iGluRs, is expressed broadly
73 in various sensory neurons, and is deeply conserved in protostomes. These findings
74 suggest that IR25a is likely to function as a co-receptor with other IRs, similar to the
75 OR83b pairing with other olfactory receptors (ORs).
76 In this study, we aimed to identify and characterize a sensilla-rich sensory
77 organ in *T. mercedesae* using scanning electron microscopy (SEM). By comparing the
78 transcriptomes of forelegs and hindlegs (the 2nd-4th legs), we identified potential genes
79 that may be highly expressed in the sensory organ. Identification of this major sensory
80 organ and its associated proteins in *T. mercedesae* inform our understanding of the
81 mechanisms of sensory perception in honey bee parasitic mites.
82
83 **Results**
84 **Identification of a sensilla-rich sensory organ on the foreleg tarsus of *T. mercedesae***
85 We observed the forelegs and hindlegs of *T. mercedesae* using SEM and found that only
86 the foreleg tarsus contained a putative sensory organ on the dorsal side, with more than
87 20 sensilla of various shapes and sizes (Fig. 1A-D). Most of the sensilla were equipped
88 with well-defined sockets (Fig. 1A). We characterized the shape of each sensillum at
89 high magnification and found that they could be classified into four different types
90 based on the shape: type 1 had a rough surface, e.g., #3 (Fig. 1E), type 2 had a terminal
91 pore, e.g., #18 (Fig. 1F), type 3 included sensilla with a smooth surface, e.g., #8 (Fig.
92 1G), and type 4 had surface pores at various densities—sensilla #2, #7, and #10 had
93 pores at high, medium, and low density, respectively (Fig. 1H-J). Several long sensilla
94 were found on all legs and these are likely to be mechanosensory bristles.
95 **Identification of potential mRNAs enriched with the sensory organ**
96 To identify potential mRNAs highly expressed in the sensory organ, we obtained
97 RNA-seq reads from the forelegs, hindlegs, and main bodies (without legs) and then
98 identified the differentially expressed genes (DEGs) between the forelegs and hindlegs.
99 Since only foreleg tarsi were equipped with the sensory organs, we expected the DEGs
100 to represent the sensory organ-associated mRNAs. We found that 46.1-83.9% of the
101 sequence reads were aligned with the *T. mercedesae* genome (Table S1) and we used
102 these to identify DEGs between the forelegs and hindlegs, the forelegs and main bodies,
103 and the hindlegs and main bodies. The lists of DEGs are shown in Tables S2, S3, and

bioRxiv preprint doi: https://doi.org/10.1101/505529; this version posted December 24, 2018. The copyright holder for this preprint (which was not certified by peer review) is the author/funder. All rights reserved. No reuse allowed without permission.

104 S4. Tables 1, S5, and S6 indicate gene ontology (GO) terms enriched for the genes
105 highly expressed in the forelegs compared to the hindlegs and main bodies, and the ones
106 highly expressed in the hindlegs relative to the main bodies, respectively. For the genes
107 highly expressed in the forelegs, many of the GO terms were associated with ion
108 channel activity, particularly iGluR activity, as well as microtubule motor activity in the
109 "Molecular function" category. In the "Biological process" category, GO terms related
110 to cilium assembly, microtubule-based processes, and detection of chemical stimulus
111 involved in sensory perception were most prevalent. All GO terms in the "Cellular
112 component" category were related to cilium, intraciliary transport particle, and BBSome
113 (Table 1). Several GO terms related to mitochondrial activity were also enriched in the
114 forelegs, compared with the main bodies, and this was similar for the genes highly
115 expressed in the hindlegs relative to the main bodies (Tables S5 and S6). These results
116 are consistent with the finding that the sensory organ on the foreleg tarsus had many
117 sensilla (Fig. 1) and with the ciliated sensory neurons and the expression of abundant
118 iGluR mRNAs. It is likely that higher expression of mRNA of genes involved in
119 mitochondrial activity in the legs relative to the main bodies would be necessary to
120 supply energy for leg movement.

121 In addition to iGluRs, the forelegs expressed high levels of transient receptor
122 potential channel A1 (as previously reported by Dong et al. [37], anoctamin-7 (TMEM16
123 family), and two gustatory receptors (GRs): Tm03548 and Tm05586 [37] (Table S2 and
124 Fig. 2). Orthologs of these GRs were also present in *Ixodes scapularis*, but were not
125 found in *D. melanogaster*, indicating that they are specifically expanded in the Acari
126 lineage. Thus, the *T. mercedesae* sensory organ appears to be equipped with various
127 sensory proteins with ion channel activity.

128 **Conserved sensory functions between *D. melanogaster* and *T. mercedesae* IR25a**
129 **and IR93a**

130 We previously annotated eight IR and 33 iGluR genes in the *T. mercedesae* genome and
131 showed that two IR mRNAs, *Tm15229* and *Tm15231*, are abundantly expressed in the
132 forelegs, using qRT-PCR [37]. These two genes are included in the above DEGs and we
133 also found that mRNAs for two non-NMDA iGluRs (Tm15234 and Tm15241), as well
134 as two other IRs (Tm15230 and Tm15243), were also highly expressed in the forelegs
135 (Fig. 2). Thus, a small fraction of iGluRs and half of IRs appear to play roles in mite
136 sensory perception.

137 Based on the phylogenetic tree of *T. mercedesae* IR and iGluR genes, together
138 with those of *D. melanogaster* and *Ixodes scapularis* [37], we found only two (out of
139 eight) IRs (*Tm15229* and *Tm15231*) were conserved, having the *D. melanogaster*

bioRxiv preprint doi: https://doi.org/10.1101/505529; this version posted December 24, 2018. The copyright holder for this preprint (which was not certified by peer review) is the author/funder. All rights reserved. No reuse allowed without permission.

140 orthologs, *IR93a* and *IR25a*, respectively. DmIR93a and DmIR25a have been shown to
141 play roles in temperature and humidity preferences [33,35,36]. To test whether the sensory
142 functions of IR93a and IR25a are deeply conserved between fruit flies and mites, we
143 first obtained the full length cDNAs of *Tm15229* and *Tm15231* by determining both the
144 5' and 3' end sequences using RACE methods. Tm15229 (TmIR93a) and Tm15231
145 (TmIR25a) share the same protein domains with DmIR93a and DmIR25a, respectively
146 (Fig. 3). Tm/DmIR25a contains the N-terminal leucine/isoleucine/valine-binding
147 protein (LIVBP)-like domain and PBP2_iGluR domain. Meanwhile, Tm/DmIR93a
148 contained only the PBP2_iGluR domain. The protein expression was confirmed by
149 ectopic expression in HEK293 cells, followed by western blot (Fig. S1). We then
150 compared the thermotactic behavior of *D. melanogaster IR93a* and *IR93a* mutants
151 expressing *TmIR93a* under *DmIR25a-Gal4* with the wild type. Expression of *DmIR93a*
152 and *DmIR25a* overlapped in the antennae [35]. We also analyzed *D. melanogaster IR25a*
153 and *IR25a* mutants expressing *DmIR25a* or *TmIR25a* under *DmIR25a-Gal4*. From our
154 assay to test thermotactic behavior, the fraction of animals in the area with temperatures
155 <24 °C significantly increased in both *IR93a* and *IR25a* mutants compared with the wild
156 type; however, expression of *TmIR93a*, *TmIR25a,* or *DmIR25a* rescued this behavioral
157 defect (Fig. 4A).
158 We then tested the humidity preferences of the fruit fly stocks described above.
159 Wild type flies preferred high (saturated NaCl, 70%) over low (saturated LiCl, 20%)
160 humidity but this preference was significantly impaired in *IR25a* and *IR93a* mutants, as
161 previously reported [33,35,36,38]. However, we did not detect humidity preference defect
162 with *IR93a* mutant. Expression of *DmIR25a* or *TmIR25a* was able to rescue the
163 humidity preference defect of the mutant fly (Fig. 4B). These results demonstrate that
164 the structures and physiological functions of IR25a and IR93a are highly conserved
165 between *D. melanogaster* and *T. mercedesae*.
166
167 **Discussion**
168 **Morphology and structure of the *T. mercedesae* sensory organ**
169 We aimed to identify a sensilla-rich sensory organ in the body of *T. mercedesae* using
170 SEM and found two such organs, one on the mouth parts and the other on the dorsal
171 side of the foreleg tarsus. The latter is comparable to Haller's organ in ticks, which is
172 considered to be responsible for detecting humidity, temperature, and odor [39,40]. Similar
173 sensory organs have also been identified in the foreleg tarsi of the mites *Dermanyssus*
174 *prognephilus* [41], *Dermanyssus gallinae* [42], and *V. destructor* [26,27]. Thus, acarids are
175 likely to share the same mechanisms for sensory perception. Nevertheless, structural

bioRxiv preprint doi: https://doi.org/10.1101/505529; this version posted December 24, 2018. The copyright holder for this preprint (which was not certified by peer review) is the author/funder. All rights reserved. No reuse allowed without permission.

176 diversity exists between different species. For example, *V. destructor* has nine large
177 sensilla (R1-9) at the periphery and nine small sensilla (S1-9) on the inside of the
178 sensory organ [26,27]. The sensory organ of *T. mercedesae* did not have such organization
179 and the localization of small and long sensilla was also random (Fig. 1). The existence
180 of four different types of sensilla appears to be shared between *T. mercedesae* and *D.*
181 *gallinae,* suggesting that the mite sensory organ could respond to mechanical stimuli,
182 humidity, temperature, and odor. Electrophysiological characterization of each
183 sensillum is, of course, necessary to support this hypothesis.

184 ***T. mercedesae* sensory organ enriched with mRNAs for sensory proteins and**
185 **proteins necessary for ciliary biogenesis/transport**

186 We sought to identify mRNAs differentially expressed in the forelegs of mites as
187 candidates for those expressed in the sensory organs. Although we have no direct
188 evidence to show that these mRNAs are indeed expressed in the sensory organ, their
189 specific existence in the forelegs, as well as the identified DEGs, support this approach.
190 The same method was used with two tick species, *Dermacentor variabilis* and *Ixodes*
191 *scapularis*, to identify mRNAs associated with the Haller's organ [43,44]. Our results to
192 show the enrichment of *TmIR25a* and *TmIR93a* mRNAs in the forelegs of *T.*
193 *mercedesae* are consistent with the results for *I. scapularis* [44]. Eliash et al. [45] also
194 reported that the *V. destructor* homolog of IR25a (this may not be the ortholog since it
195 does not have the N-terminal LIVBP domain) was highly expressed in the forelegs.
196 These results suggest that IR25a and IR93a may represent the major thermo- and
197 hygroreceptors in acarids, based on their physiological roles in fruit flies. This
198 hypothesis was further supported by our finding that TmIR25a rescued the defective
199 thermo- and hygrosensations in *D. melanogaster IR25a* mutant and TmIR93a rescued
200 the defective thermosensation in *D. melanogaster IR93a* mutant (Fig. 4). It is notable
201 that not only the structure, but also the physiological roles, have been deeply conserved
202 during Arthropod evolution [30]. *T. mercedesae* also showed high expression of two
203 acarid-specific IR mRNAs, Tm15230 and Tm15243, in the forelegs and these may
204 function as chemoreceptors. Two (Tm03548 and Tm05586) and eight GR mRNAs were
205 highly expressed in the sensory organs of *T. mercedesae* and *I. scapularis*, respectively
206 [44]. However, these GRs do not appear to be orthologs and Josek et al. [44] reported that
207 the expression of other *I. scapularis* GRs was too low to make a comparison between
208 the forelegs and hindlegs. Furthermore, most of the IRs and GRs have expanded in
209 Acari in a lineage-specific manner [44,46]. Except for Gr28b in *D. melanogaster,* which
210 has an important role in thermosensation [47], GRs are generally considered to function as
211 chemoreceptors. Thus, the above two IRs and two GRs (four in total) of *T. mercedesae*

bioRxiv preprint doi: https://doi.org/10.1101/505529; this version posted December 24, 2018. The copyright holder for this preprint (which was not certified by peer review) is the author/funder. All rights reserved. No reuse allowed without permission.

212 may detect, for example, a few odorants/tastants derived from honey bee adults, larva,
213 and larval food. This is consistent with the finding that the numbers of IR and GR genes
214 in parasitic *T. mercedesae* were dramatically reduced compared to those in "free-living"
215 mites/ticks [37]. The TRPA1 channel was also enriched in the forelegs and may function
216 as a sensor to detect nociceptive stimuli (temperature and chemicals) for avoidance, as
217 previously reported [48-50]. In summary, *T. mercedesae* may depend on IR25a, IR93a, and
218 TRPA1 for thermosensation, IR25a and IR93a for hygrosensation, and two
219 acarid-specific IRs (Tm15230 and Tm15243), two acarid-specific GRs (Tm03548 and
220 Tm05586), and TRPA1 for chemosensation.
221 Another group of proteins enriched in the forelegs is associated with cilium
222 assembly and intraciliary transport processes and includes kinesin, dynein, and
223 intraflagellar transport proteins. Cilia are organelles present on the cell surface that
224 concentrate signaling molecules to organize sensory, developmental, and homeostatic
225 function. Movement of the signaling receptor from the basal body into the cilia requires
226 IFT-A and its exit depends on IFT-B and BBSome [51]. Many sensilla are present in the
227 sensory organ of *T. mercedesae* (Fig. 1) and sensory neurons associated with the
228 sensilla have a ciliated dendrite, which requires the protein complexes described above
229 to control traffic of, for example, sensory proteins. GPCRs are considered to be the
230 major target for intraciliary transport [52]; however, the four IRs of *T. mercedesae* may
231 also depend on IFT-A, IFT-B, BBSome, and other proteins for transport. Consistent
232 with the presence of few sensilla in the Haller's organs of two tick species, enrichment
233 of these mRNAs was not observed [39]. In contrast to Carr et al. [39], we did not observe
234 high expression of mRNAs for the downstream signaling pathway components of
235 sensory proteins in the forelegs of *T. mercedesae*.
236 Our study uncovers the ancient roles of IR25a and IR93a in thermo- and
237 hygrosensation of arthropods. We also found the potential roles of evolutionarily
238 conserved intraciliary transport proteins for the entry and exit of sensory proteins in the
239 ciliated dendrites of sensory neurons. The functional disruption of these proteins could
240 be considered as an effective method to control honey bee parasitic mites as well as
241 other mites/ticks that represent major pests for plants and animals.
242

243 **Materials and Methods**

244 **Mite sampling**

245 *T. mercedesae* infested honey bee colonies were obtained from a local beekeeper in
246 Suzhou, China. Adult females of *T. mercedesae* were collected from the capped brood
247 cells and dissected under a light microscope using fine forceps. The collected mites

bioRxiv preprint doi: https://doi.org/10.1101/505529; this version posted December 24, 2018. The copyright holder for this preprint (which was not certified by peer review) is the author/funder. All rights reserved. No reuse allowed without permission.

248 were directly used for all experiments and kept together with honey bee pupae in 33 °C
249 incubator when necessary.

250 **SEM**

251 A cold field emission gun SEM (Hitachi S-4700, Hitachi Company) was used for
252 characterizing sensory organs of *T. mercedesae*. The whole mites and dissected legs
253 were sprayed with gold alloy first, and then mounted on a conductive adhesive tape.
254 During the observation, each sensillum was assigned with a number to classify the types
255 of sensilla.

256 **RNA-seq**

257 Total RNA was extracted from the forelegs, hindlegs, and main bodies of 50 adult
258 females of *T. mercedesae* using TRI Reagent (Sigma). High-quality RNA samples in
259 duplicate were then sequenced at BGI (Shenzhen, China) using Illumina HiSeq 4000
260 platform. After sequencing, the raw data were filtered to remove the adaptor sequences,
261 contamination, and low-quality reads by BGI. The Quality control (QC) was further
262 analyzed using FastQC.

263 **Bioinformatics**

264 The reference genome and annotated genes of *T. mercedesae* were first acquired from
265 NCBI (https://www.ncbi.nlm.nih.gov/genome/53919?genome_assembly_id=313451),
266 and then used for building the index by Hisat2–build indexer [53]. The generated index
267 files were used to align the clean reads of six RNA-seq samples to the reference genome.
268 Subsequently, SAM file outputs from the previous step were sorted using SAMtools [54].
269 HTSeq-count [55] was further applied to obtain the raw read counts for downstream
270 analysis of identifying the DEGs in *R* (V3.4.3) based Bioconductor edgeR package
271 (V3.20.9) [56]. DEGs were cut-off by a False Discovery Rate (FDR) at 0.05, and then they
272 were subjected to gene ontology (GO) term enrichment analysis using Blast2GO [57]. The
273 results of GO enrichment analysis between the forelegs, hindlegs as well as main bodies
274 were cut-off by FDR at 0.05.

275 ***TmIR25a* and *TmIR93a* cDNA cloning**

276 For *TmIR25a* and *TmIR93a*, the full length cDNAs were obtained by identifying the 5'
277 and 3' ends with RACE method. To amplify 5' end sequence of *TmIR25a*, the following
278 two primers: 5'-GAGTGTTTGTCCAAGTACATTCTCGA-3' (1st PCR) and
279 5'-AGTGTTATCACAAGGAGATATGAGATC-3' (2nd PCR) were used for 5'RACE
280 with SMART RACE kit (TAKARA). The 3'end sequence was determined by 3'RACE
281 using the following two primers: 5'-CCATCAAGAACATCGGTGGTG-3' (1st PCR)
282 and 5'-GGCCTGCATCACATTAGTGTTC-3' (2nd PCR). 5'RACE for *TmIR93a* was
283 conducted with two primers, 5'-ATCGAGTGCGATCACAAGCAG-3' (1st PCR) and

bioRxiv preprint doi: https://doi.org/10.1101/505529; this version posted December 24, 2018. The copyright holder for this preprint (which was not certified by peer review) is the author/funder. All rights reserved. No reuse allowed without permission.

5’-ACTCTCAGATTCCGGATTCACC-3’ (2nd PCR) using 5'-Full RACE Kit (TAKARA). For the 3’ RACE, two following two primers: 5’-GGGCAAACAGGTTACAGCTTC-3’ (1st PCR) and 5’-CCCCAACAGGACCGATCTTAT-3’ (2nd PCR) were used. *TmIR25a* full length cDNA was amplified by nested PCR using the following primer sets: Forward-5’-GCGTGAACACATCAGGCCGCT-3’ and Reverse-5’-CCCACTCGGAACTTCGTGTCG-3’ (1st PCR), Forward-5’-TTTGCGGCCGCT**ATG**TGGGTCCCTTTACGGATCTC-3’ and Reverse-5’-TTTTCTAGACTTTTCTTTTGTGGCATGTGGTCTTTC-3’ (2nd PCR). Similarly, *TmIR93a* full length cDNA was obtained using the following primer sets: Forward-5’-GGGAGAAAGCCGAGCTGGTAA-3’ and Reverse-5’-TTGTGAATGTCGCCGGTATCC-3’ (1st PCR), Forward-5’-TTTGCGGCCGCGAC**ATG**TGGCCTCGACTCATATTT-3’ and Reverse-5’-TTTTCTAGACTGTATCGCCTGGCGGGGTAGTT-3’ (2nd PCR). The PCR products were digested by NotI and XbaI and cloned into pAc5.1/V5-His vector (Thermo Fisher Scientific) in which *Drosophila melanogaster Act5C* promoter was replaced by CMV promoter for expression of the V5-epitope tagged proteins in HEK293 cells. To generate *UAS-TmIR25a* and *UAS-TmIR93a* transgenic fruit flies, the untagged versions of above expression constructs were first prepared. The EcoRI-XbaI fragment of *TmIR25a* in above construct was replaced with the restriction enzyme digested PCR product obtained with two primers, 5’-GCCACGATGACCAACTGTGAT-3’ and 5’-CGGGCCCTCTAGA**CTA**TTTCTT-3’. The HindIII-XbaI fragment of *TmIR93a* was replaced with the restriction enzyme digested PCR product obtained with two primers, 5’-GGCCAAGCGGTCATCGAGATA-3’ and 5’-GCCCTCTAGA**CTA**GTATCGCCT-3’. The untagged cDNAs were then cloned in pUASTattB [58] digested with NotI and XbaI. The accession numbers for *TmIR25a* and *TmIR93a* are LC438511 and LC438512, respectively.

Western blot

HEK293 cells in 12-well plate were transfected with 1 µg of above expression construct (the V5-epitope tagged version) using 2 µL of Lipofectamine 2000 under OPTI-MEM medium (Thermo Fisher Scientific) for 24 h. The transfected cells were washed once with PBS, and then lysed with 200 µL of SDS-PAGE sample buffer. The cell lysates were sonicated and heated at 60 °C for 5 min. The proteins were separated by 8% SDS-PAGE and transferred to a NC membrane (PALL, 66485) by Pierce 2 Fast Blotter (Thermo Fisher Scientific, B103602038). The membrane was first blocked with 5%

bioRxiv preprint doi: https://doi.org/10.1101/505529; this version posted December 24, 2018. The copyright holder for this preprint (which was not certified by peer review) is the author/funder. All rights reserved. No reuse allowed without permission.

320 BSA/TBST (10 mM Tris-HCl, 150 mM NaCl, and 0.1% Tween 20) for 40 min, and
321 then incubated with rabbit anti-V5-epitope antibody (SIGMA) (1:1000) for 2 h at room
322 temperature. The membrane was washed with TBST for five times (5 min each), and
323 then incubated with IRDye800-conjugated secondary antibody (LI-COR) (1:10,000) for
324 1.5 h at room temperature under dark and washed as above. The fluorescent signal was
325 detected by Odyssey (LI-COR).

326 **Fruit fly genetics**

327 *UAS-TmIR25a* and *UAS-TmIR93a* prepared above were integrated at attP2 site on 3rd
328 chromosome. Stocks of *IR25a-GAL4* (BDSC 41728), *IR25a*^{2} (BDSC 41737),
329 *UAS-IR25a* (BDSC 41747) and *IR93a*^{MI05555} (BDSC 42090) were obtained from
330 Bloomington Drosophila Stock Center (BDSC). Using above stocks, we generated
331 *IR25a*^{2} *UAS-IR25a, IR25a*^{2} *IR25a-GAL4, IR25a*^{2}*; UAS-TmIR25a, IR25a-GAL4;*
332 *IR93a*^{MI05555}, and *IR93a*^{MI05555} *UAS-TmIR93a* stocks. The appropriate crosses were
333 made between *Gal4* and *UAS* stocks to test whether *TmIR25a* or *TmIR93a* can rescue
334 the behavioral defects of *IR25a* or *IR93a* mutant.

335 **Thermotaxis test**

336 To assay the temperature preference of fruit flies, a temperature gradient of 10-40 °C
337 with a slope of 1.07 °C/cm was produced in an aluminum block (27 long × 15 wide ×
338 2.5 cm high) as previously reported [59]. The temperature gradient was established using a
339 cold circulating water chamber and a hot probe at each end. The aluminum block was
340 covered with moist paper to maintain a uniform relative humidity along the gradient.
341 This paper was divided into 20 observation fields with a black pencil for recording the
342 distribution of fruit flies. A glass plate with three separate lanes was placed 5 mm above
343 the block, creating suitable corridors for fruit flies to migrate. Approximately 30 adult
344 flies (4-5 days old) per lane were placed in the middle of testing arena around 25 °C
345 between the aluminum block and the glass plate, allowed to migrate for 3 h, and
346 photographed every 10 min with a digital camera. When the positions of fruit flies in
347 the apparatus were stabilized between 1.5 to 2.5 h (This time period did not differ
348 between the experimental groups), the number of fruit flies located at the area < 26 °C
349 was counted. Preference index was calculated by the number of flies at < 26 °C/the total
350 number of flies. The preference indexes of all tested groups were statistically analyzed
351 by one-way ANOVA with multiple comparisons followed by Dunnett test. In each test,
352 wild type, mutant, and the recued fruit flies were examined simultaneously. All
353 experiments were performed in a room where the temperature was kept constant at
354 25°C.

355 **Humidity preference test**

bioRxiv preprint doi: https://doi.org/10.1101/505529; this version posted December 24, 2018. The copyright holder for this preprint (which was not certified by peer review) is the author/funder. All rights reserved. No reuse allowed without permission.

356 Hygrosensory behavior was assayed as previously reported [36]. A 12-well cell culture
357 plate was modified to make a well-defined chamber with two spaces. A half of wells
358 was filled with saturated solution of LiCl (20 % humidity at 25 °C) while another half
359 was filled with saturated NaCl (70 % humidity at 25 °C) to maintain stable relative
360 humidity (RH) on the liquid surface in an enclosed space. The plate was then covered
361 by a nylon mesh and closed with a lid matching the plate. In each test, approximately 80
362 adult flies (4-5 days old) were briefly ice anesthetized and placed at the center of
363 apparatus. The lid was sealed to stabilize RH inside the apparatus. Humidity preference
364 of the fruit flies with different genotypes were recorded using a digital camera and the
365 numbers of flies on each side were recorded manually at 3-5 h after the start of
366 recording. Humidity preference index was calculated by (the number of flies on NaCl
367 side - the number of flies on LiCl side)/total number of flies. The preference indexes of
368 all tested groups were statistically analyzed by one-way ANOVA with multiple
369 comparisons followed by Dunnett test.

370

371 **References**

372

373 1 Goulson, D., Nicholls, E., Botías, C. & Rotheray, E. L. Bee declines driven by
374 combined stress from parasites, pesticides, and lack of flowers. *Science* **347**,
375 1255957, (2015).
376 2 Klein, A. M. *et al.* Importance of pollinators in changing landscapes for world
377 crops. *Proc Biol Sci* **274**, 303-313, (2007).
378 3 Aizen, M. A. & Harder, L. D. The global stock of domesticated honey bees is
379 growing slower than agricultural demand for pollination. *Curr Biol* **19**, 915-918,
380 (2009).
381 4 Evans, J. D. & Schwarz, R. S. Bees brought to their knees: microbes affecting
382 honey bee health. *Trends Microbiol* **19**, 614-620, (2011).
383 5 Rosenkranz, P., Aumeier, P. & Ziegelmann, B. Biology and control of Varroa
384 destructor. *Journal of Invertebrate Pathology* **103**, S96-S119, (2010).
385 6 de Miranda, J. R. & Genersch, E. Deformed wing virus. *Journal of Invertebrate*
386 *Pathology* **103**, S48-S61, (2010).
387 7 Martin, S. J. *et al.* Global Honey Bee Viral Landscape Altered by a Parasitic
388 Mite. *Science* **336**, 1304, (2012).
389 8 Anderson, D. L. & Morgan, M. J. Genetic and morphological variation of
390 bee-parasitic Tropilaelaps mites (Acari: Laelapidae): new and re-defined species.
391 *Exp Appl Acarol* **43**, 1-24, (2007).

bioRxiv preprint doi: https://doi.org/10.1101/505529; this version posted December 24, 2018. The copyright holder for this preprint (which was not certified by peer review) is the author/funder. All rights reserved. No reuse allowed without permission.

392 9 Luo, Q. H. *et al.* Prevalence, intensity and associated factor analysis of
393 Tropilaelaps mercedesae infesting Apis mellifera in China. *Exp Appl Acarol* **55**,
394 135-146, (2011).
395 10 Anderson, D. & Roberts, J. Standard methods for Tropilaelaps mites research.
396 *Journal of Apicultural Research* **52**, (2013).
397 11 Sammataro, D., Gerson, U. & Needham, G. Parasitic mites of honey bees: life
398 history, implications, and impact. *Annu Rev Entomol* **45**, 519-548, (2000).
399 12 Dainat, B., Ken, T., Berthoud, H. & Neumann, P. The ectoparasitic mite
400 Tropilaelaps mercedesae (Acari, Laelapidae) as a vector of honeybee viruses.
401 *Insectes Sociaux* **56**, 40-43, (2009).
402 13 Yue, C. & Genersch, E. RT-PCR analysis of Deformed wing virus in honeybees
403 (Apis mellifera) and mites (Varroa destructor). *J Gen Virol* **86**, 3419-3424,
404 (2005).
405 14 Forsgren, E., de Miranda, J. R., Isaksson, M., Wei, S. & Fries, I. Deformed wing
406 virus associated with Tropilaelaps mercedesae infesting European honey bees
407 (Apis mellifera). *Exp Appl Acarol* **47**, 87-97, (2009).
408 15 Wu, Y., Dong, X. & Kadowaki, T. Characterization of the Copy Number and
409 Variants of Deformed Wing Virus (DWV) in the Pairs of Honey Bee Pupa and
410 Infesting Varroa destructor or Tropilaelaps mercedesae. *Frontiers in*
411 *microbiology* **8**, 1558-1558, (2017).
412 16 Nazzi, F. & Le Conte, Y. Ecology of Varroa destructor, the Major Ectoparasite
413 of the Western Honey Bee, Apis mellifera. *Annu Rev Entomol* **61**, 417-432,
414 (2016).
415 17 Dainat, B., Evans, J. D., Chen, Y. P., Gauthier, L. & Neumann, P. Dead or alive:
416 deformed wing virus and Varroa destructor reduce the life span of winter
417 honeybees. *Appl Environ Microbiol* **78**, 981-987, (2012).
418 18 Khongphinitbunjong, K., Neumann, P., Chantawannakul, P. & Williams, G. R.
419 The ectoparasitic mite Tropilaelaps mercedesae reduces western honey bee,
420 Apismellifera, longevity and emergence weight, and promotes Deformed wing
421 virus infections. *J Invertebr Pathol* **137**, 38-42, (2016).
422 19 Le Conte, Y., Arnold, G. & Desenfant, P. Influence of Brood Temperature and
423 Hygrometry Variations on the Development of the Honey Bee Ectoparasite
424 Varroa jacobsoni (Mesostigmata: Varroidae). *Environmental Entomology* **19**,
425 1780-1785, (1990).
426 20 Le Conte, Y. & Arnold, G. *Etude du thermopreferendum de Varroa jacobsoni*
427 *Oud*. Vol. 19 (1988).

bioRxiv preprint doi: https://doi.org/10.1101/505529; this version posted December 24, 2018. The copyright holder for this preprint (which was not certified by peer review) is the author/funder. All rights reserved. No reuse allowed without permission.

428 21 Le Conte, Y. & Arnold, G. Influence de l'age des abeilles et de la chaleur sur le
429 comportement de *Varroa jacobsoni*. *Apidologie* **18**, 305-320, (1987).
430 22 Nazzi, F. & Conte, Y. L. Ecology of Varroa destructor, the Major Ectoparasite
431 of the Western Honey Bee, Apis mellifera. *Annual Review of Entomology* **61**,
432 417-432, (2016).
433 23 Kraus, B. Preferences of Varroa jacobsoni for honey bees (Apis mellifera L.) of
434 different ages. *Journal of Apicultural Research* **32**, 57-64, (1993).
435 24 Xie, X., Huang, Z. Y. & Zeng, Z. Why do Varroa mites prefer nurse bees?
436 *Scientific Reports* **6**, 28228, (2016).
437 25 Aumeier, P., Rosenkranz, P. & Francke, W. *Cuticular volatiles, attractivity of*
438 *worker larvae and invasion of brood cells by Varroa mites. A comparison of*
439 *Africanized and European honey bees*. Vol. 12 (2002).
440 26 Dillier, F. X., Fluri, P. & Imdorf, A. Review of the orientation behaviour in the
441 bee parasitic mite Varroa destructor: Sensory equipment and cell invasion
442 behaviour. *Revue suisse de zoologie*. **113**, 857-877, (2006).
443 27 Häußermann, C. K., Ziegelmann, B., Bergmann, P. & Rosenkranz, P. Male
444 mites (Varroa destructor) perceive the female sex pheromone with the sensory
445 pit organ on the front leg tarsi. *Apidologie* **46**, 771-778, (2015).
446 28 Belozerov, V., Kok, D. & Fourie, L. J. *Regeneration of Haller's sensory organ*
447 *in the tick, Ixodes rubicundus (Acari: Ixodidae)*. Vol. 21 (1997).
448 29 Iovinella, I. *et al.* Proteomic analysis of chemosensory organs in the honey bee
449 parasite Varroa destructor: A comprehensive examination of the potential
450 carriers for semiochemicals. *Journal of Proteomics* **181**, 131-141, (2018).
451 30 Croset, V. *et al.* Ancient Protostome Origin of Chemosensory Ionotropic
452 Glutamate Receptors and the Evolution of Insect Taste and Olfaction. *PLOS*
453 *Genetics* **6**, e1001064, (2010).
454 31 Rytz, R., Croset, V. & Benton, R. Ionotropic receptors (IRs): chemosensory
455 ionotropic glutamate receptors in Drosophila and beyond. *Insect Biochem Mol*
456 *Biol* **43**, 888-897, (2013).
457 32 Benton, R., Vannice, K. S., Gomez-Diaz, C. & Vosshall, L. B. Variant
458 ionotropic glutamate receptors as chemosensory receptors in Drosophila. *Cell*
459 **136**, 149-162, (2009).
460 33 Ni, L. *et al.* The Ionotropic Receptors IR21a and IR25a mediate cool sensing in
461 Drosophila. *Elife* **5**, (2016).
462 34 Frank, D. D. *et al.* Early Integration of Temperature and Humidity Stimuli in the
463 Drosophila Brain. *Current biology : CB* **27**, 2381-2388.e2384, (2017).

bioRxiv preprint doi: https://doi.org/10.1101/505529; this version posted December 24, 2018. The copyright holder for this preprint (which was not certified by peer review) is the author/funder. All rights reserved. No reuse allowed without permission.

464 35 Knecht, Z. A. *et al.* Distinct combinations of variant ionotropic glutamate
465 receptors mediate thermosensation and hygrosensation in Drosophila. *eLife* **5**,
466 e17879, (2016).
467 36 Enjin, A. *et al.* Humidity Sensing in Drosophila. *Curr. Biol.* **26**, 1352-1358,
468 (2016).
469 37 Dong, X. *et al.* Draft genome of the honey bee ectoparasitic mite, Tropilaelaps
470 mercedesae, is shaped by the parasitic life history. *GigaScience* **6**, 1-17, (2017).
471 38 Knecht, Z. A. *et al.* Ionotropic Receptor-dependent moist and dry cells control
472 hygrosensation in Drosophila. *eLife* **6**, e26654, (2017).
473 39 Carr, A. L. *et al.* Tick Haller's Organ, a New Paradigm for Arthropod Olfaction:
474 How Ticks Differ from Insects. *International journal of molecular sciences* **18**,
475 1563, (2017).
476 40 Leonovich, S. A. in *Sensory Systems and Communication in Arthropods*
477 44-48 (Springer, 1990).
478 41 Davis, J. C. & Camin, J. H. Setae of the Anterior Tarsi of the Martin Mite,
479 Dermanyssus prognephilus (Acari: Dermanyssidae). *Journal of the Kansas*
480 *Entomological Society* **49**, 441-449, (1976).
481 42 Cruz, M. D. S. *et al.* Scanning electron microscopy of foreleg tarsal sense organs
482 of the poultry red mite, Dermanyssus gallinae (DeGeer) (Acari:Dermanyssidae).
483 *Micron* **36**, 415-421, (2005).
484 43 Mitchell, R. D., 3rd *et al.* Infrared light detection by the haller's organ of adult
485 american dog ticks, Dermacentor variabilis (Ixodida: Ixodidae). *Ticks and*
486 *tick-borne diseases* **8**, 764-771, (2017).
487 44 Josek, T., Walden, K. K. O., Allan, B. F., Alleyne, M. & Robertson, H. M. A
488 foreleg transcriptome for Ixodes scapularis ticks: Candidates for chemoreceptors
489 and binding proteins that might be expressed in the sensory Haller’s organ. *Ticks*
490 *and Tick-borne Diseases* **9**, 1317-1327, (2018).
491 45 Eliash, N. *et al.* Chemosensing of honeybee parasite, Varroa destructor:
492 Transcriptomic analysis. *Scientific Reports* **7**, 13091, (2017).
493 46 Eyun, S.-i. *et al.* Evolutionary History of Chemosensory-Related Gene Families
494 across the Arthropoda. *Molecular Biology and Evolution* **34**, 1838-1862, (2017).
495 47 Ni, L. *et al.* A gustatory receptor paralogue controls rapid warmth avoidance in
496 Drosophila. *Nature* **500**, 580-584, (2013).
497 48 Peng, G. *et al.* TRPA1 Channels in Drosophila and Honey Bee Ectoparasitic
498 Mites Share Heat Sensitivity and Temperature-Related Physiological Functions.
499 *Frontiers in physiology* **7**, 447-447, (2016).

bioRxiv preprint doi: https://doi.org/10.1101/505529; this version posted December 24, 2018. The copyright holder for this preprint (which was not certified by peer review) is the author/funder. All rights reserved. No reuse allowed without permission.

500 49 Peng, G. *et al.* Plant-Derived Tick Repellents Activate the Honey Bee
501 Ectoparasitic Mite TRPA1. *Cell Reports* **12**, 190-202, (2015).
502 50 Dong, X. *et al.* Isoform-specific modulation of the chemical sensitivity of
503 conserved TRPA1 channel in the major honeybee ectoparasitic mite,
504 Tropilaelaps mercedesae. *Open biology* **6**, 160042, (2016).
505 51 Nachury, M. V. The molecular machines that traffic signaling receptors into and
506 out of cilia. *Current Opinion in Cell Biology* **51**, 124-131, (2018).
507 52 Schou, K. B., Pedersen, L. B. & Christensen, S. T. Ins and outs of GPCR
508 signaling in primary cilia. *EMBO reports* **16**, 1099-1113, (2015).
509 53 Kim, D., Langmead, B. & Salzberg, S. L. HISAT: a fast spliced aligner with low
510 memory requirements. *Nature Methods* **12**, 357, (2015).
511 54 Li, H. *et al.* The Sequence Alignment/Map format and SAMtools.
512 *Bioinformatics (Oxford, England)* **25**, 2078-2079, (2009).
513 55 Anders, S., Pyl, P. T. & Huber, W. HTSeq--a Python framework to work with
514 high-throughput sequencing data. *Bioinformatics (Oxford, England)* **31**, 166-169,
515 (2015).
516 56 Robinson, M. D., McCarthy, D. J. & Smyth, G. K. edgeR: a Bioconductor
517 package for differential expression analysis of digital gene expression data.
518 *Bioinformatics (Oxford, England)* **26**, 139-140, (2010).
519 57 Conesa, A. *et al.* Blast2GO: a universal tool for annotation, visualization and
520 analysis in functional genomics research. *Bioinformatics* **21**, 3674-3676, (2005).
521 58 Brand, A. H. & Perrimon, N. Targeted gene expression as a means of altering
522 cell fates and generating dominant phenotypes. *Development* **118**, 401-415,
523 (1993).
524 59 Sayeed, O. & Benzer, S. Behavioral genetics of thermosensation and
525 hygrosensation in Drosophila. *Proceedings of the National Academy of Sciences*
526 *of the United States of America* **93**, 6079-6084, (1996).
527
528
529
530
531

bioRxiv preprint doi: https://doi.org/10.1101/505529; this version posted December 24, 2018. The copyright holder for this preprint (which was not certified by peer review) is the author/funder. All rights reserved. No reuse allowed without permission.

532 **Table 1 GO terms enriched with genes highly expressed in the forelegs compared**
533 **with hindlegs of *T. mercedesae***
534

GO ID	GO name	GO category	FDR	P-value
GO:0005272	sodium channel activity	Molecular function	1.83E-09	8.77E-13
GO:0004970	ionotropic glutamate receptor activity	Molecular function	5.02E-06	1.05E-08
GO:0005234	extracellularly glutamate-gated ion channel activity	Molecular function	0.00237124	1.68E-05
GO:0008527	taste receptor activity	Molecular function	0.00237124	1.90E-05
GO:0008017	microtubule binding	Molecular function	0.02302381	2.36E-04
GO:1990939	ATP-dependent microtubule motor activity	Molecular function	0.02706201	2.86E-04
GO:0006814	sodium ion transport	Biological process	3.93E-07	3.78E-10
GO:0050912	detection of chemical stimulus involved in sensory perception of taste	Biological process	0.00237124	1.90E-05
GO:1905515	non-motile cilium assembly	Biological process	0.00237124	1.90E-05
GO:0042073	intraciliary transport	Biological process	0.00237124	1.90E-05
GO:0010378	temperature compensation of the circadian clock	Biological process	0.02706201	2.86E-04
GO:0030990	intraciliary transport particle	Cellular component	0.00237124	1.90E-05
GO:0034464	BBSome	Cellular component	0.01633013	1.60E-04

535

536

bioRxiv preprint doi: https://doi.org/10.1101/505529; this version posted December 24, 2018. The copyright holder for this preprint (which was not certified by peer review) is the author/funder. All rights reserved. No reuse allowed without permission.

537 **Figure legends**

538

539 **Figure 1 Scanning electron micrographs of *Tropilaelaps mercedesae* sensory organ.**
540 (A) The foreleg with the numbered sensilla. (B) The second leg. (C) The third leg. (D)
541 The fourth leg. (E) Sensillum #3 with a rough surface. (F) Sensillum #18 with a
542 terminal pore. (G) Sensillum #8 with a smooth surface. (H) Sensillum #2 with surface
543 pores of high density. (I) Sensillum #7 with surface pores of medium density. (J)
544 Sensillum #10 with surface pores of low density. A scale represents 50 μm in the panels
545 A-D, 2 μm in the panels H and J, and 1 μm in the panels E-G and I.

546

547 **Figure 2 Expression of ionotropic receptors (IRs), NMDA iGluRs, non-NMDA**
548 **iGluRs, and gustatory receptors (GRs) mRNAs in the forelegs, hindlegs, and main**
549 **body of *T. mercedesae*.**
550 The level of expression of each mRNA in the forelegs, hindlegs, and main body is
551 shown by a graded color (red to green) based on the counts per million mapped reads
552 (CPM).

553

554 **Figure 3 Protein domains in Dm/TmIR25a and Dm/TmIR93a**
555 Tm/DmIR25a contains a leucine/isoleucine/valine-binding protein (LIVBP)-like
556 domain at the N-terminus and PBP2_iGluR domain (ligand-binding and ion channel
557 domains) similar to iGluRs. Tm/DmIR93a contains only the PBP2_iGluR domain
558 similar to other IRs.

559

560 **Figure 4 *TmIR25a* and *TmIR93a* rescue the behavioral defects of *Drosophila***
561 ***melanogaster IR25a* and *IR93a* mutants**
562 (A) The fraction of wild type, $IR25a^2$, $IR25a^2$ expressing either *DmIR25a*
563 (*IR25a>DmIR25a*; $IR25a^2$) or *TmIR25a* (*IR25a>TmIR25a*; $IR25a^2$), $IR93a^{MI0555}$, and
564 $IR93a^{MI0555}$ expressing *TmIR93a* (*IR25a>TmIR93a*; $IR93a^{MI0555}$) under *IR25a-Gal4* in
565 the area < 24 °C of the thermal gradient. The recording was repeated 7-21 times for
566 each genotype. The mean value with error bar (± SEM) is shown for each genotype.
567 Asterisks (* and **) are significantly different from wild type, and *P*-values for $IR25a^2$
568 and $IR93a^{MI0555}$ are < 0.03 and < 0.000002, respectively. (B) Moist preference (70 over
569 20 % humidity) of fruit flies of above genotypes is shown. The recording was repeated
570 3-9 times for each genotype. The mean value with error bar (± SEM) is shown for each
571 genotype. Asterisks (**) is significantly different from wild type (*P*-value < 0.000002).

572

bioRxiv preprint doi: https://doi.org/10.1101/505529; this version posted December 24, 2018. The copyright holder for this preprint (which was not certified by peer review) is the author/funder. All rights reserved. No reuse allowed without permission.

573 **Figure S1 Expression of TmIR25a and TmIR93a proteins.**
574 The IR proteins (V5-epitope) and β-actin expressed in HEK293 cells transfected with
575 empty vector (Mock), TmIR25a-, and TmIR93a-expressing constructs were analyzed by
576 western blot. The size (kD) of protein molecular weight marker (MW) is at the left.
577

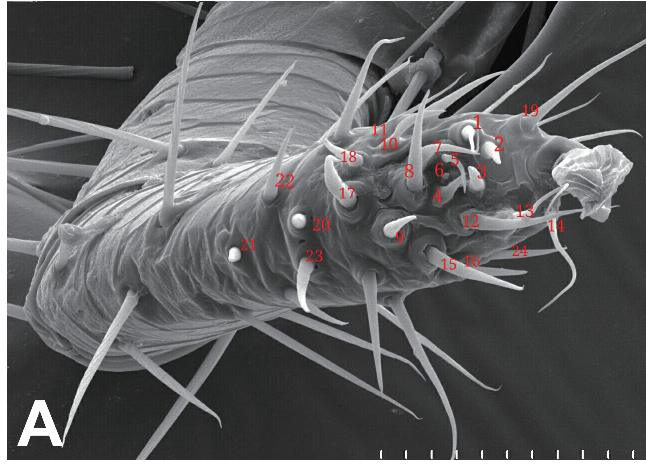
A
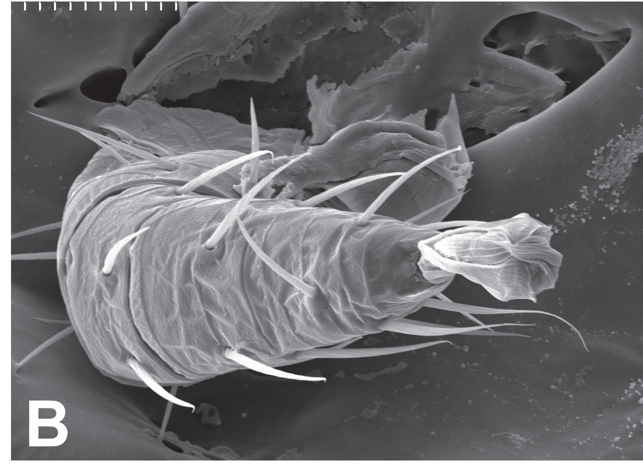
B
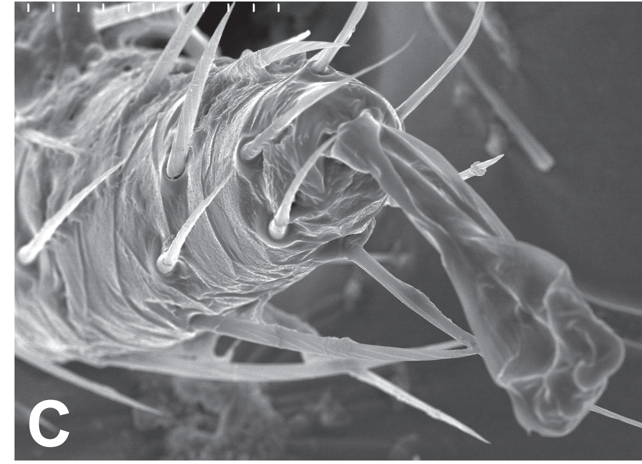
C
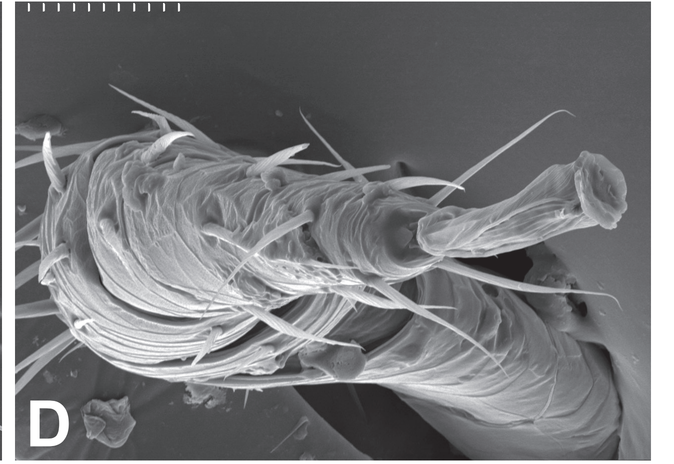
D
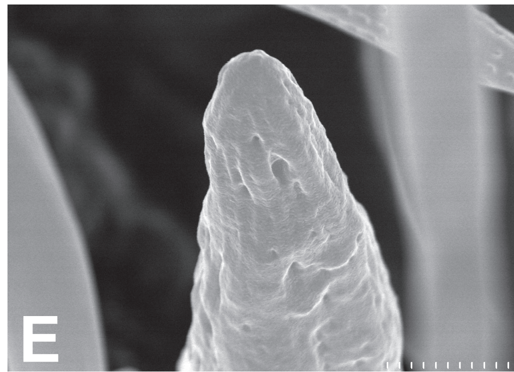
E
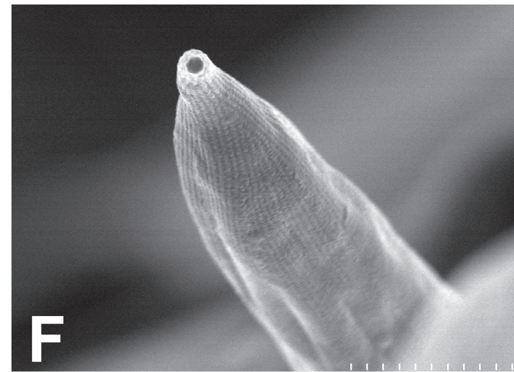
F
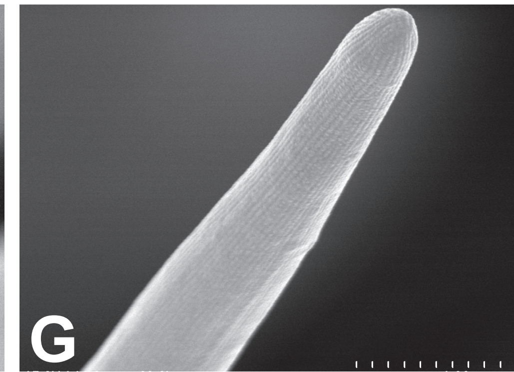
G
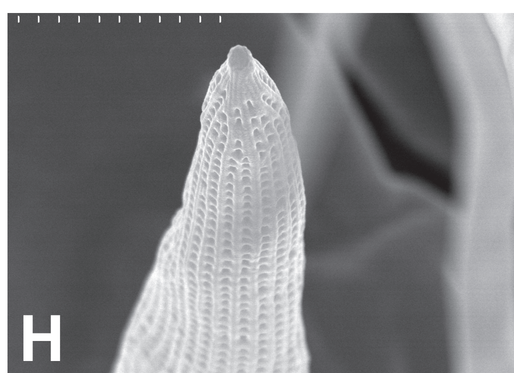
H
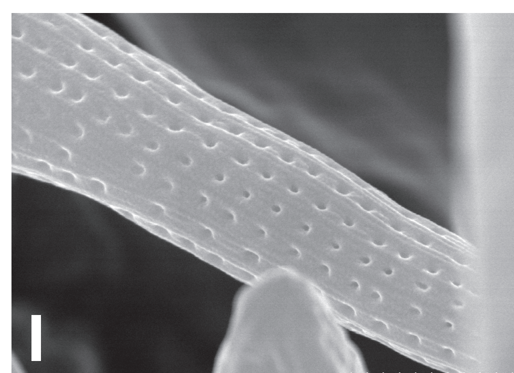
I
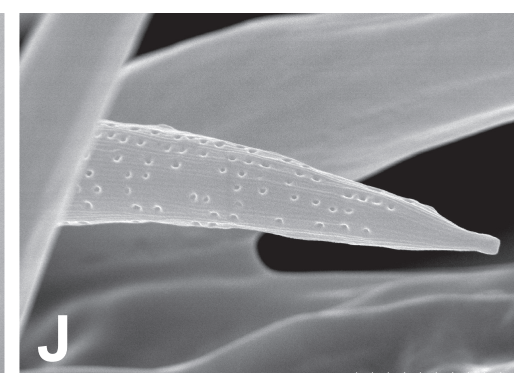
J

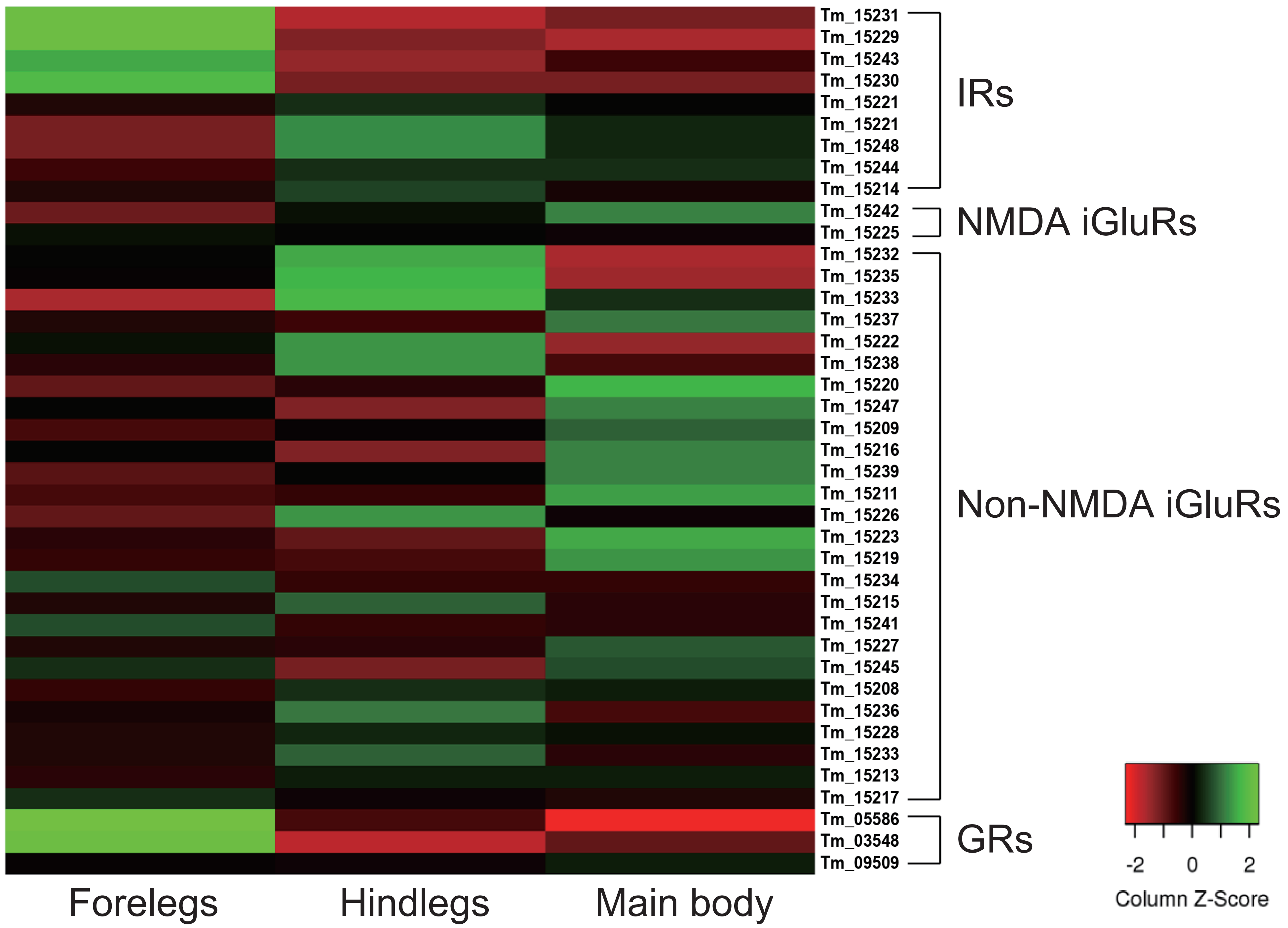
Tm_15231
Tm_15229
Tm_15243
Tm_15230
Tm_15221
Tm_15221
Tm_15248
Tm_15244
Tm_15214
Tm_15242
Tm_15225
Tm_15232
Tm_15235
Tm_15233
Tm_15237
Tm_15222
Tm_15238
Tm_15220
Tm_15247
Tm_15209
Tm_15216
Tm_15239
Tm_15211
Tm_15226
Tm_15223
Tm_15219
Tm_15234
Tm_15215
Tm_15241
Tm_15227
Tm_15245
Tm_15208
Tm_15236
Tm_15228
Tm_15233
Tm_15213
Tm_15217
Tm_05586
Tm_03548
Tm_09509
IRs
NMDA iGluRs
Non-NMDA iGluRs
GRs
-2
0
2
Column Z-Score
Forelegs
Hindlegs
Main body

Dm/TmIR25a
LIVBP
PBP2_iGluR

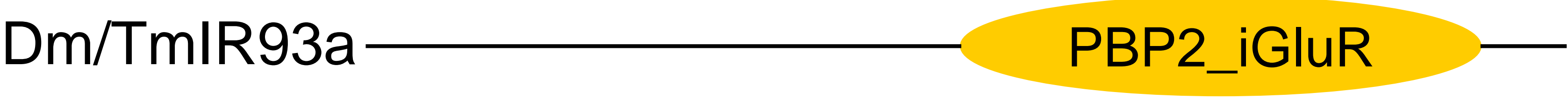
Dm/TmIR93a
PBP2_iGluR

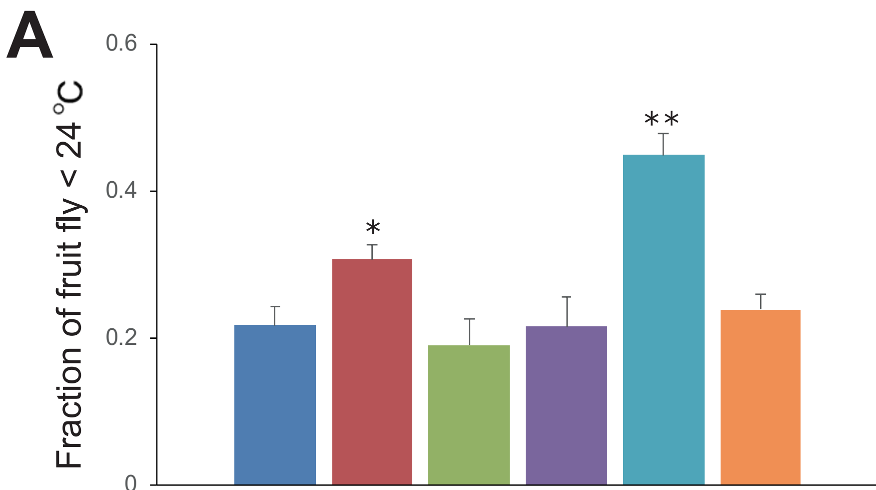
A
Fraction of fruit fly < 24 °C
0.6
0.4
0.2
0
*
**
B
Moist preference
0.8
0.6
0.4
0.2
0
**
Wild type
IR25a2
IR25a>DmIR25a; IR25a2
IR25a>TmIR25a; IR25a2
IR93aMI0555
IR25a>TmIR93a; IR93aMI0555

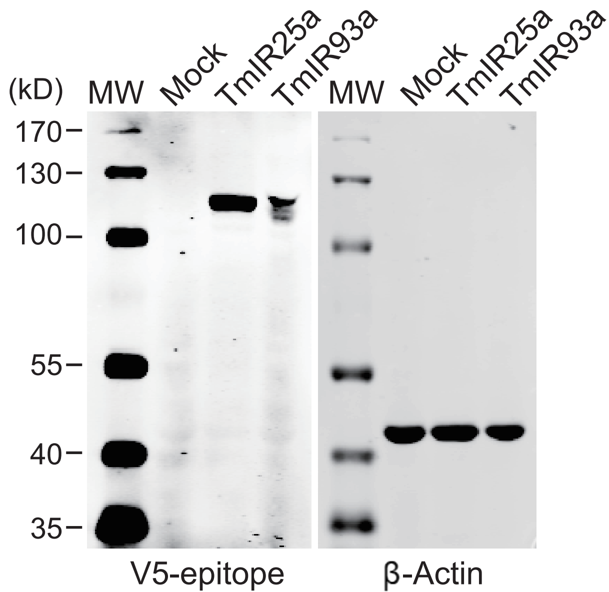
(kD)
MW
Mock
TmIR25a
TmIR93a
MW
Mock
TmIR25a
TmIR93a
170
130
100
55
40
35
V5-epitope
β-Actin